NeuroImage 184 (2019) 101–108

Contents lists available at ScienceDirect

NeuroImage

journal homepage: www.elsevier.com/locate/neuroimage

Functional MRS with J-edited lactate in human motor cortex at 4 T

Yury Koush [a,b,*], Robin A. de Graaf [a,b,c], Lihong Jiang [a,b], Douglas L. Rothman [a,b,c], Fahmeed Hyder [a,b,c,*]

[a] Magnetic Resonance Research Center, Yale University, New Haven, CT, USA
[b] Department of Radiology & Biomedical Imaging, Yale University, New Haven, CT, USA
[c] Department of Biomedical Engineering, Yale University, New Haven, CT, USA

ARTICLE INFO

Keywords:
Aerobic glycolysis
Energy metabolism
Functional MRS
Lactate
β-hydroxybutyrate
Glutamate-glutamine cycling
Neuroimaging
Oxidative phosphorylation
Finger tapping
Motor cortex

ABSTRACT

While functional MRI (fMRI) localizes regions of brain activation, functional MRS (fMRS) provides insights into metabolic underpinnings. Previous fMRS studies detected task-induced lactate increase using short echo-time non-edited ^{1}H-MRS protocols, where lactate changes depended on accurate exclusion of overlapping lactate and lipid/macromolecule signals. Because long echo-time J-difference ^{1}H-MRS detection of lactate is less susceptible to this shortcoming, we posited if J-edited fMRS protocol could reliably detect metabolic changes in the human motor cortex during a finger-tapping paradigm in relation to a reliable measure of basal lactate. Our J-edited fMRS protocol at 4T was guided by an fMRI pre-scan to determine the ^{1}H-MRS voxel placement in the motor cortex. Because lactate and β-hydroxybutyrate (BHB) follow similar J-evolution profiles we observed both metabolites in all spectra, but only lactate showed reproducible task-induced modulation by 0.07 mM from a basal value of 0.82 mM. These J-edited fMRS results demonstrate good sensitivity and specificity for task-induced lactate modulation, suggesting that J-edited fMRS studies can be used to investigate the metabolic underpinning of human cognition by measuring lactate dynamics associated with activation and deactivation fMRI paradigms across brain regions at magnetic field lower than 7T.

1. Introduction

While functional MRI (fMRI) is used to localize regions of brain activation, functional MRS (fMRS) provides a measure of the metabolic response to functional activation. The fMRI contrast is blood oxygenation level dependent (BOLD) and relies on the paramagnetic fields generated from deoxyhemoglobin packed inside red blood cells to alter the transverse relaxation rate of tissue water protons (Hyder and Rothman, 2017). The fMRS protocol detects stimuli-induced changes in the proton resonances of metabolites, which are proportional to the activity-dependent changes. Following the initial measurements of lactate increases during visual stimulation at a low magnetic field of 2.1T (Prichard et al., 1991), systematic optimization of sensitivity and accuracy for fMRS methodology at high magnetic fields like 7T (Mekle et al., 2009; Mlynarik et al., 2006; Tkac and Gruetter, 2005) have detected stimuli-induced changes of lactate, glutamate, and ɣ-aminobutyric acid (GABA) in small voxels of the human primary visual cortex (Bednarik et al., 2015b; Lin et al., 2010, 2012; Mangia et al., 2007b, 2009; Mekle et al., 2016; Schaller et al., 2013b). Recently, smaller but reliable modulations in lactate ($17 \pm 5\%$) and glutamate ($2 \pm 1\%$) were also observed in the human motor cortex during a standard finger-tapping paradigm at 7T (Schaller et al., 2014).

These recent fMRS studies at 7T have been performed using short echo-time (TE) non-edited ^{1}H-MRS protocols. In addition, visual cortex is known to be the most reliable location in the human brain to probe with MRS protocols, often used primarily because of relative simplicity of the stimulus paradigm required to achieve robust and sustained physiological activation as well as the high signal-to-noise ratio (SNR) of detection arising from both close proximity of the visual cortex to the radio-frequency (RF) head coil elements and better shimming conditions. Because of the added SNR gain and better spectral resolution of 7T scanning, applying fMRS protocols at lower magnetic fields and/or other brain areas is not usually considered (Schaller et al., 2014). While the short TE non-edited ^{1}H-MRS protocol is advantageous because of high SNR, the precise assessment of changes in lactate (or other metabolites) is contingent on deconvolution of the overlapping signals from lipids/macromolecules and lactate.

Because long TE J-difference ^{1}H-MRS detection of lactate intrinsically removes overlapping signals, we posited if J-edited fMRS at 4T

* Corresponding authors. Magnetic Resonance Research Center, Yale University, 300 Cedar Street, New Haven, CT 06519, USA.
E-mail addresses: yury.koush@yale.edu (Y. Koush), fahmeed.hyder@yale.edu (F. Hyder).

https://doi.org/10.1016/j.neuroimage.2018.09.008
Received 28 July 2018; Received in revised form 31 August 2018; Accepted 4 September 2018
Available online 8 September 2018

could reliably detect lactate modulations in the human motor cortex during a finger-tapping paradigm. Spectral editing with J modulation takes advantage of the quantum mechanical properties of specific molecules to "edit" them from the overall ^{1}H-MRS spectrum (Rothman et al., 1984), thereby providing separation of lactate from overlapping resonances and/or lipids/macromolecules. However, J-editing is vulnerable to subtraction errors due to motion, which can obscure small changes in the lactate signal. In this study, we used long TE J-edited ^{1}H-MRS to selectively and reproducibly detect lactate changes during physiological stimulation. Through post-processing optimization, we were able to obtain the sensitivity and subtraction accuracy needed to measure even small changes in lactate. Furthermore, we were able to obtain macromolecule-free measurements of lactate at rest, which allowed an unambiguous determination of the percentage increase in the lactate signal as well as potentially important information on the pre-stimulus rest state. We tested the sensitivity of J-editing for changes in lactate (vs. β-hydroxybutyrate (BHB)) at 4T through conventional finger-tapping that exerts stable BOLD signal changes in the primary motor cortex.

2. Methods

2.1. Participants

Ten healthy volunteers (right-handed, 9 male, 1 female, age 36.5 ± 3.8) participated in the experiment that consisted of one fMRI run and from two to four fMRS runs spanning over two to four days (in total 28 runs, 2.8 ± 0.2 runs per subject, one fMRS run per daily session). All participants gave their consent to participate in the study in accordance with procedures approved by the Yale University Human Investigation Committee. The experiments were performed at the Magnetic Resonance Research Center on a 4T Bruker spectrometer using a 16-channel transmit-receive head coil. Before the experiment participants received the instructions that they will perform a conventional finger-tapping experiment to activate their motor cortex. The instructions included an explanation of the task conditions, and that they have to fixate at the central fixation dot, breathe steadily and remain as still as possible throughout the experiment.

2.2. fMRI and fMRS experiments

The experimental session of the first day consisted of an fMRI localizer run and a single fMRS run. During the subsequent daily sessions over the next three days participants performed one to three fMRS runs. We ran a finger-tapping fMRI localizer to delineate the primary motor cortex region-of-interest (ROI), which consisted of five 97 s finger-tapping blocks interleaved with five 97 s fixation blocks (16.2 min in total). Participants were asked to perform a visually cued finger-to-thumb tapping task at a rate of 3 Hz for both hands, which provides stable and high primary motor cortex activation (Schaller et al., 2014; Vafaee and Gjedde, 2004; Vafaee et al., 2012). During finger-tapping blocks participants were asked to follow carefully the flashing numbers from 1 to 4 (indicated above the fixation dot) for each of four fingers alternating to the thumb. During fixation blocks (cued with 'FIX' above the fixation dot) participants were asked to stop tapping.

The fMRS run consisted of three 333 s finger-to-thumb tapping blocks for both hands interleaved with three 333 s fixation blocks (33.3 min in total). Visual cues and instructions were displayed using a rectangular projection screen at the rear of the scanner bore using a mirror positioned within the head-coil. Practice sessions outside the scanner ensured a proper tapping performance at the given 3 Hz frequency, which was also carefully monitored during fMRI and fMRS runs. Foam paddings were placed around the subject's head inside the head-coil to minimize head motion.

2.3. fMRI and fMRS data acquisition

We used a single-shot T_2*-weighted FLASH sequence for the functional localizer fMRI run, which was acquired during the first experimental session (74 scans, repetition time (TR) = 375.3 ms, TE = 30 ms, voxel size = 4 × 4 × 4 mm, slice gap = 1 mm, matrix size = 61 × 35 × 10, flip angle = 30°, bandwidth = 50 kHz, image acquisition time (TA) = 13.1 s, total TA = 16.2 min, 1 dummy image). Using SPM12 (www.fil.ion.ucl.ac.uk/spm), the T_2* data from the functional localizer were processed to identify the activated motor cortex ROI. An individual fMRS voxel was placed in the middle of the identified ROI to cover the activation associated with the motor and somatosensory areas. This entire process took ~15 min (for details, see *fMRI data processing* section).

We used ^{1}H J-difference editing for the fMRS scans (150 paired spectra, number of averages = 2, TR = 3330 ms, TE = 144 ms, voxel size = 22 × 28 × 22 mm, total TA = 33.3 min) with the MEscher-GArwood scheme (MEGA (Mescher et al., 1998),), which consisted of 10 ms Gaussian editing pulses with −99 Hz (5.26 ppm) and 99 Hz (4.10 ppm) offsets, and 114 Hz (0.67 ppm) bandwidth at 4T. For conventional slice selective excitation combined with localization by adiabatic selective refocusing (semi-LASER (Scheenen et al., 2008),), we used a non-adiabatic slice-selective Shinnar-Le-Roux (Pauly et al., 1991) excitation pulse (90°, 2 ms, bandwidth = 2800 Hz) followed by two pairs of the second-order hyperbolic secant adiabatic full passage pulses (Tannus and Garwood, 1996) for refocusing (180°, 4 ms, bandwidth = 5000 Hz). For water suppression we used variable pulse power with optimized relaxation delays (VAPOR (Tkac et al., 1999),) with Gaussian 15 ms pulses (bandwidth = 133.6 Hz). Prior to fMRS acquisitions, we acquired maps of the static magnetic field (B_0) and adjusted the basic frequency. We shimmed up to the second-order, both globally and locally, based on the B_0 map. We also acquired a reference water spectrum from the same fMRS voxel using the same J-editing sequence but with zero-amplitude RF pulses for the water suppression and the editing pulses (one spectrum, 10 averages). In this reference water spectrum the eddy currents were exactly the same as in the subsequent fMRS spectra, such that the water signal could later be used for eddy current corrections. We also acquired a structural scan to facilitate fMRS voxel localization with a 3D FLASH scan (TR = 20 ms, TE = 6.5 ms, voxel size = 1 × 1 × 1 mm, matrix size = 256 × 160 × 120, flip angle = 10°, bandwidth = 100 kHz, TA = 6.4 min).

To elucidate spectral overlap between lactate and BHB resonances given their similar J-evolution profiles and to ensure sensitivity of our J-editing sequence to test both molecules on our 4T scanner, we conducted experiments on a phantom consisting of NAA (10 mM), lactate (1 mM), and BHB (0.3 mM) prior to the in vivo study. The phantom was prepared with distilled deionized water and potassium hydroxide buffer (pH = 7.3 at 25 °C; Sigma Aldrich, USA). We acquired a single 33.3 min fMRS run at room temperature using the same data acquisition parameters as for the in vivo fMRS run.

2.4. fMRI data processing

Immediately after acquiring the fMRI localizer runs, the images were pre-processed with SPM12, i.e., they were realigned to the mean scan of each run and smoothed with an isotropic Gaussian kernel with an 8 mm full-width-at-half maximum. First, the dummy scan was skipped to account for T_1 saturation effects. We then used a general linear model for a whole-brain first-level analysis with separate regressors for the finger-tapping and the fixation conditions, along with covariates derived from head movement parameters to capture residual motion artifacts. The regressors were modeled as boxcar functions convolved with the canonical hemodynamic response function. To account for the relatively long image acquisition time (13.1 s) of our fMRI scans, first-level whole-brain analysis was performed slice-wise, given slice-specific shifted condition onsets, and combined into the single whole-brain statistical

activation map at the end. The motor cortex ROI was defined from the local maximum of the BOLD response as defined by the thresholded activation map (t-statistics, $p < 0.01$ unc.). The fMRS voxel was carefully placed over the fMRI-derived ROI to ensure that the voxel captures the entire activation pattern while at the same time it does not capture signal from outside the brain (Bednarik et al., 2015b; Koush et al., 2011, 2013, 2014; Mangia et al., 2007b; Schaller et al., 2014). The fMRS voxel coordinates were transferred from the FLASH scan space to the single MRS voxel space given the specifications of the Bruker coordinate system.

For the subsequent fMRS daily sessions, we first ran a template FLASH fMRI scan and then co-registered the first day average fMRI scan (i.e., the scan in the space of which the ROI was identified) to this template together with the prescribed ROI. By this procedure, the coordinates of the first-day ROI localization in the MRS spaces were transferred to the current day MRS space. The registration of the fMRI data was performed using conventional spatial registration routines, default parameters, and precision settings as determined by SPM12.

2.5. fMRS data (pre)processing

The in vitro spectra were processed by the same steps as described for the in vivo spectra. For the in vivo data we first preprocessed the spectroscopic data per fMRS run and then derived quantitative estimates per finger-tapping and fixation blocks, and participants, respectively. The FIDs from each coil in the 16-channel array were weighted by the SNR of the water signals and then added together (Roemer et al., 1990). The resultant 300 FIDs underwent several preprocessing and processing steps (de Graaf, 2007). The preprocessing included subsequent frequency drift correction, eddy current correction, automatic spectra phase correction, spectra alignment, J-edited grouping, and apodization. For the frequency drift correction, we used the run-average NAA peak as a reference peak and aligned the frequency of all the subsequent NAA peaks to it. Subsequently, eddy current correction of each spectrum per run was performed using the phase evolution of the acquired reference water FID (Klose, 1990; Tkac and Gruetter, 2005). Next, separately for each fMRS run, we performed a zero-order phase correction of the eddy current corrected spectra based on the phase-nulling offset defined from the run-averaged NAA peak. To define the phase-nulling offset, i.e., the phase required to be added/subtracted from the initial spectrum to reach the symmetricity of its imaginary part, we phase-alternated the run-average NAA spectrum. For phase alterations, we gradually added extra phase offset to the initial spectrum in the range from 0° to 360°, with 1° steps. For the symmetricity criteria, we computed an average of the absolute sums of all positive values and all negative values from the imaginary spectrum part given the NAA peak window (2.01 ± 0.25 ppm). The resultant averages (i.e., per gradual phase) formed a phase vector with extremums where the phase-altered spectrum was symmetrical. Phase-nulling offset was defined by the maximum symmetricity value and a positive real spectrum. This phase offset was applied to all the spectra within the run.

Subsequently, each of the run spectra was aligned prior to averaging, and each of the 150-paired spectra (i.e., J-edited spectra pairs acquired in an interleaved order) was aligned to each other. Next, the aligned paired spectra were summed to form a J-edited sum spectrum and subtracted to form a J-edited difference spectrum. The frequency drift correction and spectra alignment procedures outlined above were performed using NAA peak as a reference and a parametric least-square fitting approach to fit each spectrum to the reference spectrum given prescribed precision levels and modeled spectra amplitude, phase, and frequency. Finally, 2×150 grouped J-edited spectra (i.e., 150 summed spectra and 150 difference spectra) were apodized using 2 Hz Gaussian and 2 Hz exponential filters.

Preprocessed summed and difference J-edited spectra were averaged per each finger-tapping and fixation blocks, and per finger-tapping and fixation conditions across blocks and across runs, respectively. The spectra were scaled with the scaling factor 0.01. For illustration purposes, we also averaged all finger-tapping and fixation spectra across all acquired runs to get illustrative spectra per group for both conditions and differences between the conditions. Since each spectra averaging slightly affects the reference spectra frequency and shape, frequency drift and shape alignments were performed after each averaging.

To diminish the BOLD effect in the J-edited difference spectra, finger-tapping summed spectra were first centered and then fit to the average spectrum for the fixation condition. We used spectra shape alignment and fitting procedures as described above, and extended it with an extra exponential term to model the BOLD-induced linewidth modulations. Such estimated spectra shift and linewidth modulations were applied to both finger-tapping J-edited summed and difference spectra, which were corrected for the linewidth changes due to the BOLD effect.

Since lactate and BHB have similar J-evolution profiles and their resonances overlap partly, we estimated their levels based on the linear combination model (LC model) quantification (Provencher, 2001). The basis set of the simulated lactate and BHB metabolites was used to fit the differential spectra over a range of 0.6–1.9 ppm. The high bandwidth of the refocusing pulses (5000 Hz) relative to the chemical shift difference of the lactate/BHB resonances (475 Hz at 4T) leads to a minimal chemical shift displacement, thereby avoiding the need for spatially-resolved basis set simulations (Edden and Barker, 2011; Yablonskiy et al., 1998). To approximate the NAA linewidth modulations by the finger-tapping condition, we used J-edited summed spectra to which BOLD compensation was not applied. We fitted the NAA peak in LC model over a range of 1.9–2.1 ppm. The contributions of potentially overlapping metabolites (glutamate, glutamine) were minimal at our echo time and were not further considered. To estimate the reference NAA levels, we performed the similar LC modeling based on the BOLD-compensated summed spectra. Conventional polynomial baseline correction was performed for the NAA and lactate/BHB peaks. The uncertainties in these quantifications were estimated by the Cramér–Rao lower bound (CRLB) procedure as previously described (Cavassila et al., 2001).

The BOLD-compensated NAA levels were used for the scaling of the lactate and BHB levels, assuming 10 mM NAA. In addition, these levels were corrected for the T_2 effect by introducing an additional T_2 scaling factor. This scaling factor was approximated as a ratio $\exp(-TE/T_{2NAA})/\exp(-TE/T_{2lactate}) = 1.13$, given $TE = 44$ ms, and $T_{2NAA} = 297$ ms and $T_{2lactate} = 239$ ms based on a recent 3T study (Madan et al., 2015).

The water spectra were preprocessed similarly to the J-edited spectra, but without 2 Hz exponential and 2 Hz Gaussian apodization. For comparison and quality assurance purposes, the water peak linewidth was assessed using LC model quantification of the water spectra and the time-domain linear approximation of the first 100 ms of the acquired FID (Koush et al., 2011, 2013, 2014). We also estimated noise in the spectrum from 10 to 11 ppm.

We used two-tailed paired t-tests to compare the metabolite levels between finger-tapping and fixation conditions. The correlation between metabolite levels was assessed using two-tailed Spearman correlation. We also assessed the linear dependencies across (i) fixation metabolite levels, (ii) finger-tapping metabolite levels, and (iii) the differences between the finger-tapping and fixation metabolite levels using one-way repeated measures analysis of variances (ANOVAs). For average values, we reported mean and standard error of the mean (SEM). The spectroscopic data were processed using custom and NMRWizard (mrrc.yale.edu) routines written in Matlab (Mathworks, MA, USA).

3. Results

We investigated a phantom solution with lactate and BHB to reveal their in vivo overlap with characteristic 6.99 and 5.6 Hz splitting, respectively (Fig. 1). The fMRS voxel placement was guided by the ROI determined from the fMRI experiment (Fig. 2A). The SNR of fMRS data, determined from the height of the NAA peak (CRLB $= 0.2 \pm 0.01$) relative to the noise peak (from 10 to 11 ppm), was 350.0 ± 18.7 ($n = 28$). The J-edited summed and difference spectra from the motor cortex (Fig. 2B and C) were acquired with the narrow group average linewidths

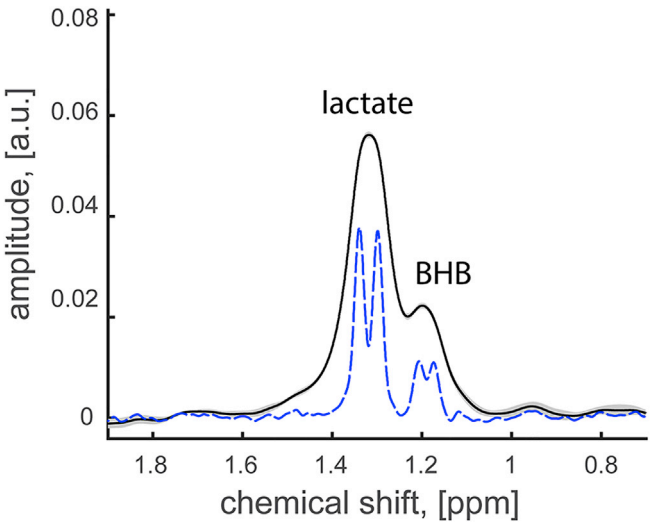

Fig. 1. J-edited spectrum of a phantom containing lactate (1.0 mM) and BHB (0.3 mM), where lactate at 1.32 ppm and BHB at 1.19 ppm were scaled to NAA (10 mM). For comparison purposes (see Fig. 3C), an extra 9.5 Hz exponential and 2 Hz Gaussian apodization was applied to the phantom spectrum (dashed blue line) to mimic line broadening observed in vivo (solid black line). The dashed blue line illustrates the characteristic 6.99 Hz splitting for lactate and 5.6 Hz splitting for BHB.

for water (5.1 ± 0.3 Hz, water CRLB = 0.3 ± 0.04), lactate, and BHB (9.7 ± 0.3 Hz, lactate CRLB = 3.6 ± 0.2, BHB CRLB = 14.6 ± 1.3) peaks. The LC modeling and time domain approximation of the water linewidth were similar (paired two-tailed *t*-test, t = 0.3, p = 0.8, df = 27) and highly correlated (two-tailed Spearman correlation, rho = 0.93, $p < 0.001$). BOLD-induced linewidth narrowing during finger-tapping was estimated from individually quantified NAA linewidth differences, i.e., between fixation and finger-tapping conditions for each fMRS run (i.e., linewidths of 6.81 ± 0.20 Hz for finger-tapping and 6.94 ± 0.27 Hz for fixation, corresponds to 0.13 ± 0.13 Hz difference for 1.9 ± 1.3% BOLD signal change from fixation).

During the finger-tapping condition compared to the fixation condition, we detected no difference between the corresponding NAA levels (two-tailed paired *t*-test, t = 0.6, p = 0.54, df = 27) and noise integrals (two-tailed paired *t*-test, t = 0.3, p = 0.80, df = 27), but a significant increase in lactate levels (two-tailed paired *t*-test, t = 2.7, p = 0.01, df = 27) (Fig. 3). The stimulation-induced lactate modulations corresponded to a change of 8.6 ± 4.0% from basal levels (0.89 ± 0.04 mM finger-tapping, and 0.82 ± 0.04 mM fixation lactate levels). Because BHB at 1.19 ppm has the same J-evolution profiles as lactate at 1.32 ppm, our J-edited spectra captured both BHB and lactate reliably in all acquisitions. However BHB levels did not show a significant increase induced by the finger-tapping (two-tailed paired *t*-test, t = 1.3, p = 0.21, df = 27; with BHB levels of 0.28 ± 0.02 mM for finger-tapping, and 0.25 ± 0.02 mM for fixation).

We ran several subjects additional times in order to assess the reproducibility of the BHB measurement which had not been previously

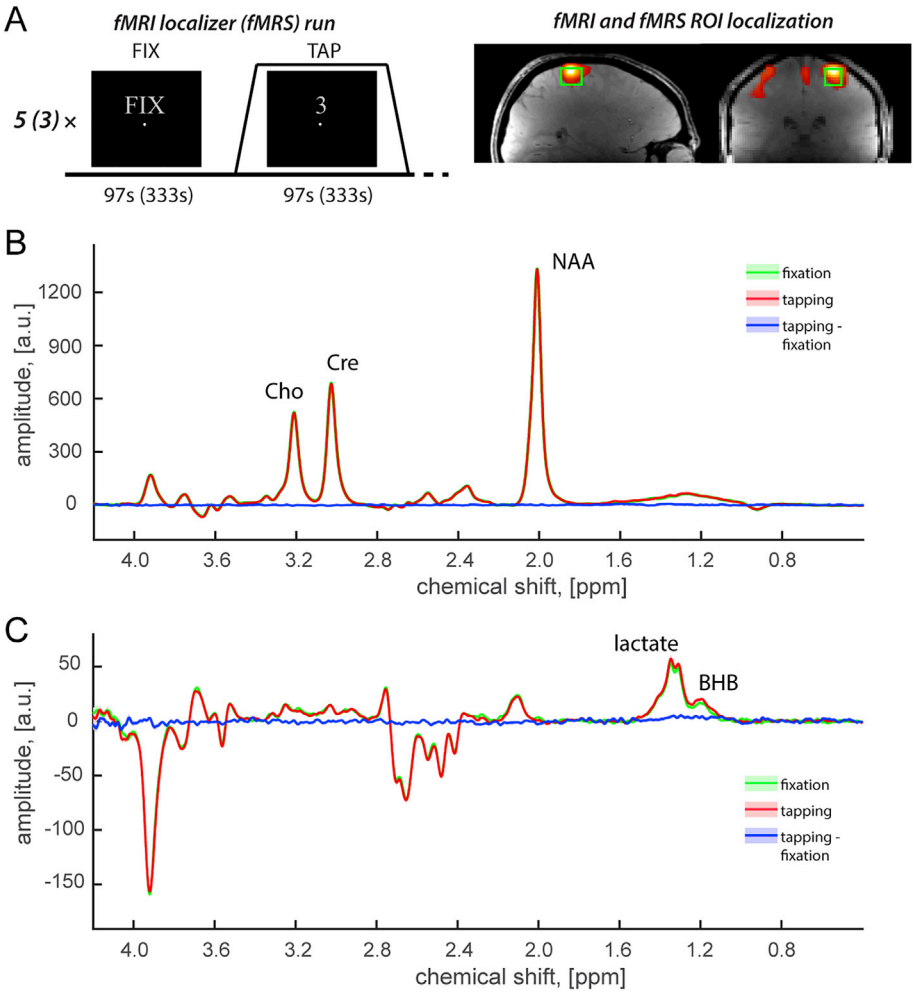

Fig. 2. The fMRI and fMRS experimental design and results. (A) An illustration of the fMRI and fMRS runs and the ROI localization (green box). Each fMRI run consisted of five 97 s finger-tapping blocks interleaved with five 97 s fixation blocks (16.2 min in total). Each fMRS run consisted of three 333 s finger-tapping blocks interleaved with three 333 s fixation blocks (33.3 min in total). For the fMRS run, the block durations are shown in brackets. The right motor cortex was localized based on the fMRI run and positioned as the single voxel for fMRS run (green box = 22 × 28 × 22 mm). FIX = fixation, TAP = finger-tapping. Group average J-edited (B) summed and (C) difference spectra for fixation (green), finger-tapping (red), and the difference (i.e., blue, which is tapping - fixation). (B) The summed spectra illustrate NAA (2.01 ppm), choline (Cho, 3.19 ppm), and creatine (Cre, 3.03 ppm) peaks, as well as lipids and macromolecule contamination (1.6–0.8 ppm). (C) The difference spectra illustrate J-edited lactate (1.32 ppm) and co-edited BHB (1.19 ppm) peaks. Shaded plots denote SEM. The sum and difference spectra were scaled with the scaling factor 0.01.

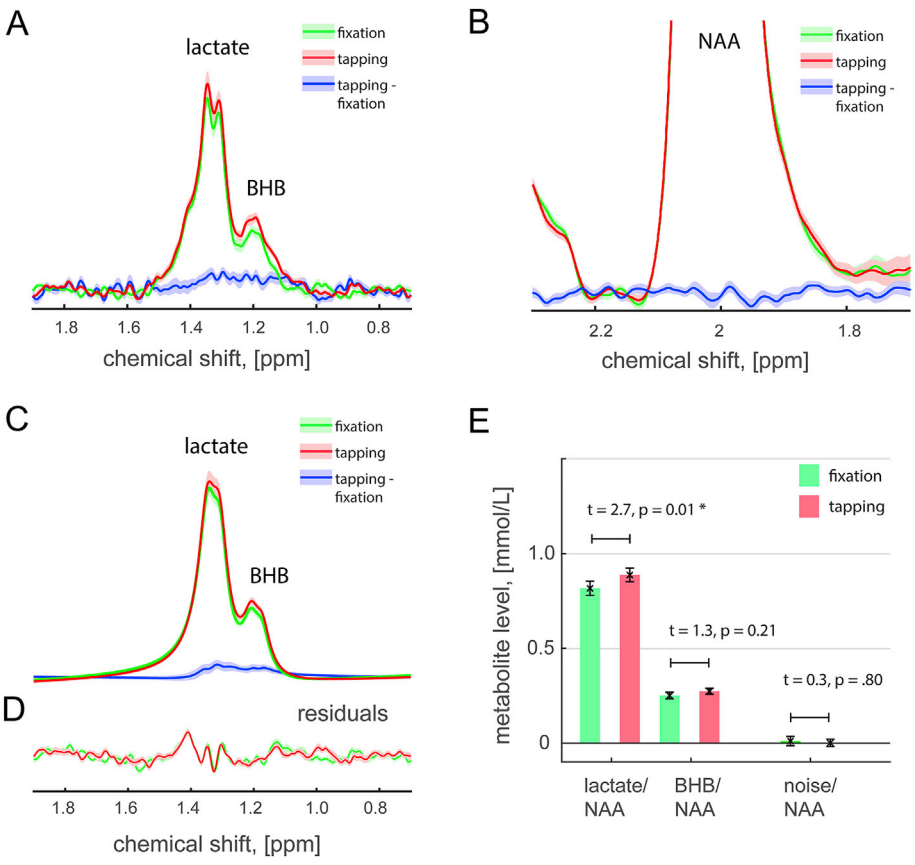

Fig. 3. Details of fMRS data for lactate, BHB, and NAA. Group average spectra of (A) lactate and BHB as well as (B) NAA are illustrated for fixation (green) and finger-tapping (red) conditions and their difference (blue). (C) Group LC modeled lactate and BHB spectra as well as (D) residuals are illustrated for fixation (green) and finger-tapping (red) conditions and their difference (blue). (E) Normalized lactate, BHB, and noise levels are shown for fixation and finger-tapping conditions, assuming NAA concentration of 10 mM. Shaded plots and error bars denote SEM.

reported in the fMRS literature. The number of runs per subject was limited by their availability. More specifically, six out of ten subjects were scanned 3–4 times, which resulted in 10 retest fMRS runs. We did not find a difference between the test (10 subjects, 18 runs) and retest (6 subjects, 10 runs) fMRS runs in terms of the baseline levels of lactate (two-tailed two-sample *t*-test, $t = 0.2$, $p = 0.86$, $df = 26$) and BHB (two-tailed two-sample *t*-test, $t = 0.7$, $p = 0.51$, $df = 26$), and thus jointly analyzed them. For test runs (10 subjects, 18 runs), we consistently found a significant increase of lactate during finger-tapping compared to fixation conditions (two-tailed paired *t*-test, $t = 2.5$, $p = 0.02$, $df = 17$; with lactate levels of 0.85 ± 0.05 mM for finger-tapping, and 0.77 ± 0.05 mM for fixation, which corresponds to a change of $10.4 \pm 6.0\%$ from basal levels), but no significant BHB increase (two-tailed paired *t*-test, $t = 1.2$, $p = 0.24$, $df = 17$; with BHB levels of 0.26 ± 0.02 mM for finger-tapping, and 0.24 ± 0.02 mM for fixation).

To investigate lactate dynamics across conditions, we averaged 150 J-edited pairs (i.e., 25 spectra per block) to a single paired spectrum per block. We did not detect a significant lactate increase with consecutive experimental conditions (Fig. 4; one-way ANOVAs; lactate fixation $F(2,81) = 0.2$, $p = 0.79$; lactate tapping $F(2,81) = 1.3$, $p = 0.28$; lactate tapping - fixation $F(2,81) = 1.2$, $p = 0.31$). We also performed a correlation analysis between the initial (i.e., first fixation block) lactate levels and the tapping-induced differences relative to the fixation level. We did not find a correlation between the initial lactate level and induced changes (two-tailed Spearman correlation, $rho = -0.22$, $p = 0.27$).

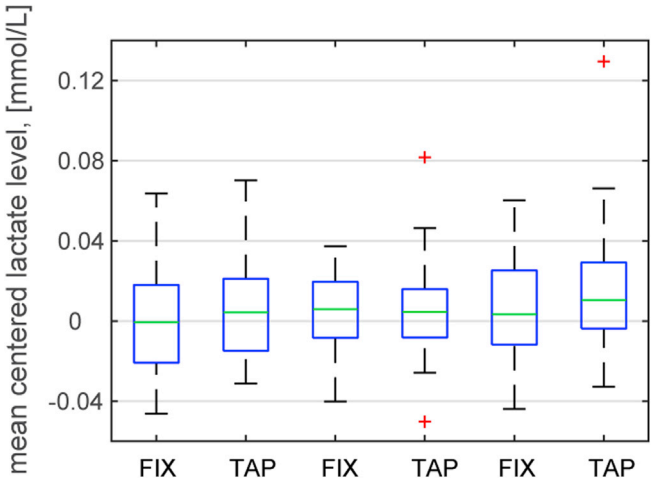

Fig. 4. Group average box plots of the mean centered lactate levels for consecutive fixation and finger-tapping blocks. The individual lactate levels were mean centered to the first fixation block lactate level. For quantified metabolite levels over time (i.e., across 3 finger-tapping blocks), we did not detect significant increase of lactate with consecutive finger-tapping conditions (one-way ANOVA; lactate fixation $F(2,81) = 0.2$, $p = 0.79$; lactate tapping $F(2,81) = 1.3$, $p = 0.28$; lactate tapping - fixation $F(2,81) = 1.2$, $p = 0.31$). The acquired 150 J-edited pairs (i.e., 25 per block) were averaged to a single paired spectrum per block. Finger-tapping induced differences were computed as the differences between absolute finger-tapping and fixation concentration levels. Symbols represent medians (green lines), lower and upper quartiles (top and bottom of blue boxes), error bars (dashed black lines), and outliers (red crosses). The box plot error bars represent the most extreme non-outlier data points, which is different from SEMs shown in Fig. 2 and 3. FIX = fixation, TAP = finger-tapping.

4. Discussion

Our J-difference editing fMRS study showed that direct observation of the functional modulation of lactate is feasible at 4T with sufficient time resolution. Using standard finger-tapping we observed significant lactate increase in the motor cortex ($8.6 \pm 4.0\%$, 0.07 ± 0.04 mM) during finger-tapping (0.89 ± 0.04 mM) as compared to the fixation (0.82 ± 0.04 mM)

condition (Fig. 3). Our results are in good agreement with the previous fMRS studies at 7T, which measured lactate increases in the motor cortex (17 ± 5% (Schaller et al., 2014), and visual cortex (7–20% (Bednarik et al., 2015b; Lin et al., 2010; Mangia et al., 2007a; Mekle et al., 2016; Schaller et al., 2013b),). Because lactate (1.32 ppm) and BHB (1.19 ppm) have similar J-evolution profiles, we were able to detect both in our edited spectra as confirmed through simulation using a model of the pure compounds (Fig. 1). In addition to the task-induced lactate modulations, we repeatedly observed BHB (Figs. 1–3). We performed LC model quantification of both molecules to delineate the extent of their overlap, which revealed significant increases of lactate, however BHB changes were not significant (Fig. 3E).

LC modeling is highly sensitive to the noise when the number of averages is reduced, and thus requires assumptions about larger CRLB threshold for data quantification (Schaller et al., 2014). Hence we favored high SNR against high temporal resolution of our data and averaged 25 spectra per block, which is sufficient to show the functional modulations in steady-state (i.e., over long 5 min periods of time), and the linear dependencies of the metabolite levels across subsequent regulation blocks. We illustrated lactate dynamics across consecutive task and rest blocks, where we found no significant linear dependencies in lactate levels with repeated stimuli (Fig. 4), and no correlation between initial and task-induced lactate level differences.

^{1}H-MRS studies at 3T and lower B_0 have shown that lactate detected with short TE are not always feasible in healthy human brain due to low lactate concentration (<1 mM) (Bednarik et al., 2015a; Terpstra et al., 2016)), although the same method reliably observed higher lactate levels in human brain tumors (~10 mM lactate at 3T (Madan et al., 2015)). High specificity for activation-induced lactate modulations in our data at 4T was maintained using long TE (144 ms) J-difference editing acquisitions. J-edited ^{1}H-MRS takes advantage of the quantum mechanical properties of lactate to specifically edit it from the overall ^{1}H-MRS spectrum (Rothman et al., 1984), providing direct insights into the overlapping resonances that appear from multiple metabolites like lipids or macromolecules. ^{1}H-MRS studies have shown that physiological modulations of lactate in the visual cortex could be observed even at 1.5T using long TE, and therefore, possesses less susceptibility to artifacts due to substantial suppression of the relatively short T_2 for the lipid and macromolecule background signals (TE = 270 ms (Kuwabara et al., 1995)). Thus our J-editing acquisitions reproducibly detected lactate modulations devoid of lipids and macromolecules, which were achieved both by the long TE and J-edited difference spectra calculation (Figs. 2 and 3). These data had high spectra SNR (350.0 ± 18.7) and sufficient temporal resolution to obtain dynamics of lactate (Fig. 4). The quality of the acquired data was assured by the narrow water linewidth (5.1 ± 0.3 Hz), low spectral noise, and low CRLB for lactate quantification (3.6 ± 0.2). A potential limitation of our protocol, however, is that the long 16 min fMRI scan acquired prior to the first day fMRS session could cause the potential problem for the subsequent J-editing data due to B_0 shifts arising from gradient heating and cooling. However in our experimental design there was about 15–25 min break between the fMRI and fMRS data acquisitions, delays attributed to fMRI data processing, fMRS voxel positioning, and conventional delays for ^{1}H-MRS adjustments. This data acquisition break substantially reduced B_0 drifts. Overall we had a 14.0 ± 1.3 Hz frequency drift over the entire 33.3 min fMRS runs, which did not significantly reduce editing efficiency. In addition to the retrospective frequency drift and phase correction used here and elsewhere (Near et al., 2015; Waddell et al., 2007), the real-time correction techniques can be implemented to counteract these shortcomings, such as the techniques based on the interleaved navigators (Henry et al., 1999; Hess et al., 2011; Keating and Ernst, 2012; Star-Lack et al., 2000; Thiel et al., 2002), the residual water signal (Helms and Piringer, 2001), and the reference peak (e.g., NAA or total Cr) locking if implemented within the real-time loop (Near et al., 2015; Waddell et al., 2007).

The BOLD-induced modulation of the NAA peak linewidth by the finger-tapping (i.e., 0.13 ± 0.13 Hz NAA linewidth difference; NAA linewidths of 6.81 ± 0.20 and 6.94 ± 0.27 Hz for finger-tapping and fixation, respectively) confirmed proper placement of fMRS voxels in the activated motor cortex area. These BOLD linewidth changes were compensated both in summed and difference J-edited spectra using NAA peak as a reference. In addition, BOLD linewidth modulations in our study (0.13 ± 0.13 Hz) were generally smaller than previous short TE (6–26 ms) non-edited ^{1}H-MRS protocols, which observed 0.25 and 0.45–0.46 Hz modulations in the motor (Schaller et al., 2014) and visual (Bednarik et al., 2015b; Schaller et al., 2013b) cortices, respectively. The reduction of the BOLD-induced NAA linewidth modulation in our data could be attributed, in part, to the relatively long TE and minimal partial volume effect. The long TE may have contributed to the reduction of the quality of our NAA-based BOLD quantifications because of reduced absolute spectra amplitude and modulations. The partial volume effect cannot be completely excluded in single voxel fMRS studies and could be expected to be larger in the motor cortex (Schaller et al., 2014). Due to the small linewidth changes from the BOLD effect under our experimental conditions (i.e., at B_0 of 4T and long TE of 144 ms), its impact on NAA and lactate quantification even without this correction would be minimal, as previously shown (Bednarik et al., 2015b; Schaller et al., 2013b, 2014). However our correction procedure effectively eliminated any BOLD influence on our results.

Despite the increased quality of fMRS data at 7T with short TE non-edited ^{1}H-MRS, there has been nearly a factor of two range for basal lactate reported - from 0.56 mM to 1.02 mM (Lin et al., 2012; Mangia et al., 2007a; Mekle et al., 2009, 2016; Schaller et al., 2013a, 2014). Similar basal lactate variations with non-edited ^{1}H-MRS have been reported at 1.5T (0.20 mM in basal ganglia (Kuwabara et al., 1995)), at 2.0T (0.38 mM in visual cortex (Frahm et al., 1996), and at 2.1T (0.71 mM in visual cortex (Prichard et al., 1991)). We suggest the variation in the measured basal lactate level is due to the lactate peak in the non-edited spectra being on the shoulder of larger lipids/macromolecule signals (Behar et al., 1994), which could affect the accuracy of the spectral fitting procedures given CRLB<20. Our measured basal lactate level at fixation value was 0.82 ± 0.04 mM (assuming 10 mM NAA), which falls within the range reported in the literature. Due to intrinsic elimination of overlapping lipids/macromolecule resonances with J-editing (the levels and composition of which may change regionally in the brain and with disease), we recommend J-editing as a way to obtain accurate basal lactate measurements, especially at lower B_0. Nevertheless, further investigations are needed to compare the long and short TE lactate quantification precision and temporal resolution of J-editing measurements. Based on our J-editing results at 4T we expect that fMRS sensitivity of results from J-editing at 7T should be further improved, but due to the long TE will be less sensitive than short TE methods for quantifying the change in lactate concentration with activation paradigms. However it may still be of use when an accurate basal measurement of lactate concentration is needed under conditions where there is ambiguity in fitting the lipids/macromolecule background signals.

Cerebral blood flow (CBF) and metabolic rates of glucose (CMR_{Glc}) and oxygen ($CMRO_2$) consumption are all tightly coupled throughout the resting human brain (Hyder et al., 2016). Thus, at rest, uniformly stable oxygen-to-glucose index (OGI = $CMRO_2/CMR_{Glc}$) and oxygen extraction fraction (OEF = $CMRO_2/(C_a \cdot CBF)$, where C_a is the arterial oxygen content) is observed in the cerebral cortex. However during physiological stimuli slight decreases in both OGI ($CMRO_2$-CMR_{Glc} uncoupling) and OEF ($CMRO_2$-CBF uncoupling) are detected from their resting values in localized brain regions (for a historical perspective see (Hyder and Rothman, 2012)).

The greater stimuli-induced rise in CBF compared to $CMRO_2$ (Fox and Raichle, 1986) is consistent with the increased BOLD effect during task compared to rest (Vafaee et al., 2012), but over two decades of assessment of stimulus-induced changes in $CMRO_2$ and CBF with calibrated fMRI experiments (Hyder and Rothman, 2017) suggest a much tighter coupling than originally reported. The slightly higher task-related

increase in CMR_{Glc} compared to $CMRO_2$ (Fox et al., 1988) suggests less efficient glucose oxidation compared to rest and some stimuli-induced lactate increase (Lin et al., 2010). Although lactate has generally been considered as an end product of glycolysis, the proposed role of lactate in metabolic processes of brain function is constantly growing. The ^{13}C-MRS in vivo data regarding the linear relationship between cerebral activity (glutamate recycling between neurons and astrocytes or glutamate-glutamine cycling) and energy metabolism (neuronal glucose oxidation) suggest that lactate can be oxidized in both neurons and astrocytes, enabling lactate to contribute to energetics during activation in both neuronal and glial compartments (Hyder et al., 2006; Sibson et al., 1997). Thus there is an increasing support for lactate being one of the major sources of energy production as compared to glucose (Hyder and Rothman, 2012; Wyss et al., 2011). Recently a novel perspective of lactate has been proposed, where it acts as a volume transmitter of cellular signals that also regulates energy metabolism in large neuronal ensembles (Bergersen and Gjedde, 2012).

In our study, we observed a steady-state finger-tapping lactate increase of 0.07 ± 0.04 mM (i.e., $8.6 \pm 4.0\%$ from basal level of 0.82 ± 0.04 mM), which indicates a sustained increased flux into the pyruvate-lactate pool and increased lactate efflux to the blood (Hyder and Rothman, 2012; Mangia et al., 2012; Schaller et al., 2014), often referred to as aerobic glycolysis. Based on our quantification of the resting lactate level, the fractional increase of lactate in aerobic glycolysis is relatively small for the finger-tapping task. However it may also play an important role in linking CBF changes to the metabolic alterations (Bergersen and Gjedde, 2012; Vafaee et al., 2012).

Interestingly, BHB could be visually identified in previously reported fMRS difference spectra (i.e., activation minus baseline), however its values were never estimated (Schaller et al., 2013b, 2014). It is known that BHB can rise substantially with exercising (Newman and Verdin, 2017) and fasting (Jiang et al., 2011). In addition, BHB could provide energy for basal and activity-dependent neuronal oxidation when supply of glucose is low for the body's energy needs (Chowdhury et al., 2014). However its potential role in acute human brain activation has never been addressed so far and requires a thorough investigation. We speculate that similarly to its conventional implication in exercising and fasting studies, BHB could serve as an alternative energy buffer recruited during raised energy demand yielded by increased brain activity when glucose supplies are low, such as during fasting.

5. Summary

Our results at 4T show that by using J-editing to improve spectral resolution it is possible to obtain high quality time courses of lactate changes during functional activation. The lactate levels in basal and stimulated conditions measured at 4T in human motor cortex with editing was similar to previous studies at 7T without editing in human visual cortex (Bednarik et al., 2015b; Mangia et al., 2012; Mekle et al., 2016; Schaller et al., 2013b) and human motor cortex (Schaller et al., 2014). By removing the overlapping signals from lipids/macromolecules the J-editing approach removes the need to deconvolve the lactate signal from overlapping nuisance resonances which may be responsible for the variation in reported basal lactate levels in previous studies while retaining good SNR for measuring dynamic changes in lactate. In addition, it allowed for the first time the examination of BHB as a fuel source during functional activation. We believe that J-edited fMRS studies will allow improved lactate measurements at B_0 in the 3T and 4T range to investigate the metabolic underpinning of human cognition by measuring lactate dynamics for activation and deactivation fMRI paradigms.

Acknowledgements

Supported by the Swiss National Science Foundation (P300PB_161083) and the National Institutes of Health of United States (R01 NS-100106, R01 MH-067528, R01 EB-014861, P30 NS-052519).

References

Bednarik, P., Moheet, A., Deelchand, D.K., Emir, U.E., Eberly, L.E., Bares, M., Seaquist, E.R., Oz, G., 2015a. Feasibility and reproducibility of neurochemical profile quantification in the human hippocampus at 3 T. NMR Biomed. 28, 685–693.
Bednarik, P., Tkac, I., Giove, F., DiNuzzo, M., Deelchand, D.K., Emir, U.E., Eberly, L.E., Mangia, S., 2015b. Neurochemical and BOLD responses during neuronal activation measured in the human visual cortex at 7 Tesla. J. Cerebr. Blood Flow Metabol. 35, 601–610.
Behar, K.L., Rothman, D.L., Spencer, D.D., Petroff, O.A., 1994. Analysis of macromolecule resonances in 1H NMR spectra of human brain. Magn. Reson. Med. 32, 294–302.
Bergersen, L.H., Gjedde, A., 2012. Is lactate a volume transmitter of metabolic states of the brain? Front. Neuroenergetics 4, 5.
Cavassila, S., Deval, S., Huegen, C., van Ormondt, D., Graveron-Demilly, D., 2001. Cramer-Rao bounds: an evaluation tool for quantitation. NMR Biomed. 14, 278–283.
Chowdhury, G.M., Jiang, L., Rothman, D.L., Behar, K.L., 2014. The contribution of ketone bodies to basal and activity-dependent neuronal oxidation in vivo. J. Cerebr. Blood Flow Metabol. 34, 1233–1242.
de Graaf, R.A., 2007. In: Vivo NMR Spectroscopy, second ed. Principles and Techniques. John Wiley & Sons, Ltd.
Edden, R.A.E., Barker, P.B., 2011. If J doesn't evolve, it won't J-resolve: J-PRESS with bandwidth-limited refocusing pulses. Magn. Reson. Med. 65, 1509–1514.
Fox, P.T., Raichle, M.E., 1986. Focal physiological uncoupling of cerebral blood flow and oxidative metabolism during somatosensory stimulation in human subjects. Proc. Natl. Acad. Sci. U. S. A. 83, 1140–1144.
Fox, P.T., Raichle, M.E., Mintun, M.A., Dence, C., 1988. Nonoxidative glucose consumption during focal physiologic neural activity. Science 241, 462–464.
Frahm, J., Kruger, G., Merboldt, K.D., Kleinschmidt, A., 1996. Dynamic uncoupling and recoupling of perfusion and oxidative metabolism during focal brain activation in man. Magn. Reson. Med. 35, 143–148.
Helms, G., Piringer, A., 2001. Restoration of motion-related signal loss and line-shape deterioration of proton MR spectra using the residual water as intrinsic reference. Magn. Reson. Med. 46, 395–400.
Henry, P.G., van de Moortele, P.F., Giacomini, E., Nauerth, A., Bloch, G., 1999. Field-frequency locked in vivo proton MRS on a whole-body spectrometer. Magn. Reson. Med. 42, 636–642.
Hess, A.T., Tisdall, M.D., Andronesi, O.C., Meintjes, E.M., van der Kouwe, A.J., 2011. Real-time motion and B0 corrected single voxel spectroscopy using volumetric navigators. Magn. Reson. Med. 66, 314–323.
Hyder, F., Herman, P., Bailey, C.J., Moller, A., Globinsky, R., Fulbright, R.K., Rothman, D.L., Gjedde, A., 2016. Uniform distributions of glucose oxidation and oxygen extraction in gray matter of normal human brain: No evidence of regional differences of aerobic glycolysis. J. Cerebr. Blood Flow Metabol. 36, 903–916.
Hyder, F., Patel, A.B., Gjedde, A., Rothman, D.L., Behar, K.L., Shulman, R.G., 2006. Neuronal-glial glucose oxidation and glutamatergic-GABAergic function. J. Cerebr. Blood Flow Metabol. 26, 865–877.
Hyder, F., Rothman, D.L., 2012. Quantitative fMRI and oxidative neuroenergetics. Neuroimage 62, 985–994.
Hyder, F., Rothman, D.L., 2017. Advances in imaging brain metabolism. Annu. Rev. Biomed. Eng. 19, 485–515.
Jiang, L., Mason, G.F., Rothman, D.L., de Graaf, R.A., Behar, K.L., 2011. Cortical substrate oxidation during hyperketonemia in the fasted anesthetized rat in vivo. J. Cerebr. Blood Flow Metabol. 31, 2313–2323.
Keating, B., Ernst, T., 2012. Real-time dynamic frequency and shim correction for single-voxel magnetic resonance spectroscopy. Magn. Reson. Med. 68, 1339–1345.
Klose, U., 1990. In vivo proton spectroscopy in presence of eddy currents. Magn. Reson. Med. 14, 26–30.
Koush, Y., Elliott, M.A., Mathiak, K., 2011. Single voxel proton spectroscopy for neurofeedback at 7 tesla. Materials 4.
Koush, Y., Elliott, M.A., Scharnowski, F., Mathiak, K., 2013. Real-time automated spectral assessment of the BOLD response for neurofeedback at 3 and 7T. J. Neurosci. Meth. 218, 148–160.
Koush, Y., Elliott, M.A., Scharnowski, F., Mathiak, K., 2014. Comparison of real-time water proton spectroscopy and echo-planar imaging sensitivity to the BOLD effect at 3 T and at 7 T. PLoS One 9, e91620.
Kuwabara, T., Watanabe, H., Tsuji, S., Yuasa, T., 1995. Lactate rise in the basal ganglia accompanying finger movements: a localized 1H-MRS study. Brain Res. 670, 326–328.
Lin, A.-L., Fox, P.T., Hardies, J., Duong, T.Q., Gao, J.-H., 2010. Nonlinear coupling between cerebral blood flow, oxygen consumption, and ATP production in human visual cortex. Proc. Natl. Acad. Sci. U. S. A. 107, 8446–8451.
Lin, Y., Stephenson, M.C., Xin, L., Napolitano, A., Morris, P.G., 2012. Investigating the metabolic changes due to visual stimulation using functional proton magnetic resonance spectroscopy at 7T. J. Cerebr. Blood Flow Metabol.: Official Journal of the International Society of Cerebral Blood Flow and Metabolism 32, 1484–1495.
Madan, A., Ganji, S.K., An, Z., Choe, K.S., Pinho, M.C., Bachoo, R.M., Maher, E.M., Choi, C., 2015. Proton T2 measurement and quantification of lactate in brain tumors by MRS at 3 Tesla in vivo. Magn. Reson. Med. 73, 2094–2099.
Mangia, S., Giove, F., Dinuzzo, M., 2012. Metabolic pathways and activity-dependent modulation of glutamate concentration in the human brain. Neurochem. Res. 37, 2554–2561.
Mangia, S., Giove, F., Tkac, I., Logothetis, N.K., Henry, P.-G., Olman, C.A., Maraviglia, B., Di Salle, F., Ugurbil, K., 2009. Metabolic and hemodynamic events after changes in

neuronal activity: current hypotheses, theoretical predictions and in vivo NMR experimental findings. J. Cerebr. Blood Flow Metabol.: Official Journal of the International Society of Cerebral Blood Flow and Metabolism 29, 441–463.
Mangia, S., Tkac, I., Gruetter, R., Van de Moortele, P.-F., Maraviglia, B., Ugurbil, K., 2007a. Sustained neuronal activation raises oxidative metabolism to a new steady-state level: evidence from 1H NMR spectroscopy in the human visual cortex. J. Cerebr. Blood Flow Metabol.: Official Journal of the International Society of Cerebral Blood Flow and Metabolism 27, 1055–1063.
Mangia, S., Tkac, I., Gruetter, R., Van de Moortele, P.F., Maraviglia, B., Ugurbil, K., 2007b. Sustained neuronal activation raises oxidative metabolism to a new steady-state level: evidence from 1H NMR spectroscopy in the human visual cortex. J. Cerebr. Blood Flow Metabol. 27, 1055–1063.
Mekle, R., Kuhn, S., Pfeiffer, H., Aydin, S., Schubert, F., Ittermann, B., 2016. Detection of metabolite changes in response to a varying visual stimulation paradigm using short-TE 1 H MRS at 7 T. NMR Biomed. 30.
Mekle, R., Mlynarik, V., Gambarota, G., Hergt, M., Krueger, G., Gruetter, R., 2009. MR spectroscopy of the human brain with enhanced signal intensity at ultrashort echo times on a clinical platform at 3T and 7T. Magn. Reson. Med. 61, 1279–1285.
Mescher, M., Merkle, H., Kirsch, J., Garwood, M., Gruetter, R., 1998. Simultaneous in vivo spectral editing and water suppression. NMR Biomed. 11, 266–272.
Mlynarik, V., Gambarota, G., Frenkel, H., Gruetter, R., 2006. Localized short-echo-time proton MR spectroscopy with full signal-intensity acquisition. Magn. Reson. Med. 56, 965–970.
Near, J., Edden, R., Evans, C.J., Paquin, R., Harris, A., Jezzard, P., 2015. Frequency and phase drift correction of magnetic resonance spectroscopy data by spectral registration in the time domain. Magn. Reson. Med. 73, 44–50.
Newman, J.C., Verdin, E., 2017. Beta-hydroxybutyrate: a signaling metabolite. Annu. Rev. Nutr. 37, 51–76.
Pauly, J., Leroux, P., Nishimura, D., Macovski, A., 1991. Parameter relations for the shinnar-leroux selective excitation pulse design algorithm. IEEE Trans. Med. Imag. 10, 53–65.
Prichard, J., Rothman, D., Novotny, E., Petroff, O., Kuwabara, T., Avison, M., Howseman, A., Hanstock, C., Shulman, R., 1991. Lactate rise detected by 1H NMR in human visual cortex during physiologic stimulation. Proc. Natl. Acad. Sci. U. S. A. 88, 5829–5831.
Provencher, S.W., 2001. Automatic quantitation of localized in vivo 1H spectra with LCModel. NMR Biomed. 14, 260–264.
Roemer, P.B., Edelstein, W.A., Hayes, C.E., Souza, S.P., Mueller, O.M., 1990. The NMR phased array. Magn. Reson. Med. 16, 192–225.
Rothman, D.L., Behar, K.L., Hetherington, H.P., Shulman, R.G., 1984. Homonuclear 1H double-resonance difference spectroscopy of the rat brain in vivo. Proc. Natl. Acad. Sci. U. S. A. 81, 6330–6334.
Schaller, B., Mekle, R., Xin, L., Kunz, N., Gruetter, R., 2013a. Net increase of lactate and glutamate concentration in activated human visual cortex detected with magnetic resonance spectroscopy at 7 tesla. J. Neurosci. Res. 91, 1076–1083.
Schaller, B., Mekle, R., Xin, L., Kunz, N., Gruetter, R., 2013b. Net increase of lactate and glutamate concentration in activated human visual cortex detected with magnetic resonance spectroscopy at 7 tesla. J. Neurosci. Res. 91, 1076–1083.
Schaller, B., Xin, L., O'Brien, K., Magill, A.W., Gruetter, R., 2014. Are glutamate and lactate increases ubiquitous to physiological activation? A (1)H functional MR spectroscopy study during motor activation in human brain at 7Tesla. Neuroimage 93 (Pt 1), 138–145.
Scheenen, T.W., Klomp, D.W., Wijnen, J.P., Heerschap, A., 2008. Short echo time 1H-MRSI of the human brain at 3T with minimal chemical shift displacement errors using adiabatic refocusing pulses. Magn. Reson. Med. 59, 1–6.
Sibson, N.R., Dhankhar, A., Mason, G.F., Behar, K.L., Rothman, D.L., Shulman, R.G., 1997. In vivo 13C NMR measurements of cerebral glutamine synthesis as evidence for glutamate-glutamine cycling. Proc. Natl. Acad. Sci. U. S. A. 94, 2699–2704.
Star-Lack, J.M., Adalsteinsson, E., Gold, G.E., Ikeda, D.M., Spielman, D.M., 2000. Motion correction and lipid suppression for 1H magnetic resonance spectroscopy. Magn. Reson. Med. 43, 325–330.
Tannus, A., Garwood, M., 1996. Improved performance of frequency-swept pulses using offset-independent adiabaticity. J. Magn. Reson. 120, 133–137.
Terpstra, M., Cheong, I., Lyu, T., Deelchand, D.K., Emir, U.E., Bednarik, P., Eberly, L.E., Oz, G., 2016. Test-retest reproducibility of neurochemical profiles with short-echo, single-voxel MR spectroscopy at 3T and 7T. Magn. Reson. Med. 76, 1083–1091.
Thiel, T., Czisch, M., Elbel, G.K., Hennig, J., 2002. Phase coherent averaging in magnetic resonance spectroscopy using interleaved navigator scans: compensation of motion artifacts and magnetic field instabilities. Magn. Reson. Med. 47, 1077–1082.
Tkac, I., Gruetter, R., 2005. Methodology of H NMR spectroscopy of the human brain at very high magnetic fields. Appl. Magn. Reson. 29, 139–157.
Tkac, I., Starcuk, Z., Choi, I.Y., Gruetter, R., 1999. In vivo 1H NMR spectroscopy of rat brain at 1 ms echo time. Magn. Reson. Med. 41, 649–656.
Vafaee, M.S., Gjedde, A., 2004. Spatially dissociated flow-metabolism coupling in brain activation. Neuroimage 21, 507–515.
Vafaee, M.S., Vang, K., Bergersen, L.H., Gjedde, A., 2012. Oxygen consumption and blood flow coupling in human motor cortex during intense finger tapping: implication for a role of lactate. J. Cerebr. Blood Flow Metabol. 32, 1859–1868.
Waddell, K.W., Avison, M.J., Joers, J.M., Gore, J.C., 2007. A practical guide to robust detection of GABA in human brain by J-difference spectroscopy at 3 T using a standard volume coil. Magn. Reson. Imaging 25, 1032–1038.
Wyss, M.T., Jolivet, R., Buck, A., Magistretti, P.J., Weber, B., 2011. In vivo evidence for lactate as a neuronal energy source. J. Neurosci. 31, 7477–7485.
Yablonskiy, D.A., Neil, J.J., Raichle, M.E., Ackerman, J.J., 1998. Homonuclear J coupling effects in volume localized NMR spectroscopy: pitfalls and solutions. Magn. Reson. Med. 39, 169–178.